Optical conductivity studies of $La_{3/2}Sr_{1/2}NiO_4$: Lattice effect on charge ordering

J. H. Jung
Center for Strongly Correlated Materials Research, Seoul National University, Seoul 151-747, Korea

D.-W. Kim* and T. W. Noh
School of Physics and Research Center for Oxide Electronics, Seoul National University, Seoul 151-747, Korea

H. C. Kim and H.-C. Ri
Material Science Laboratory, Korea Basic Science Institute, Taejeon 305-333, Korea

S. J. Levett,† M. R. Lees, D. McK. Paul, and G. Balakrishnan
Department of Physics, University of Warwick, Coventry CV4 7AL, United Kingdom
(Received 5 March 2001; published 28 September 2001)

Optical conductivity spectra $\sigma(\omega)$ of a $La_{3/2}Sr_{1/2}NiO_4$ single crystal were investigated over a wide photon energy range with variations of temperature and polarization. Strong anisotropies in phonon modes and electronic structures are observed between the ab plane ($E\|ab$) and c axis ($E\|c$). In the midinfrared region, $\sigma(\omega)$ for $E\|ab$ show several peaks due to small polaron and optical transitions between neighboring Ni sites; however, those for $E\|c$ show negligible spectral weights. By assigning proper optical transitions, the crystal field splitting energy between e_g orbitals and Hund's rule exchange energy are estimated to be around 0.7 eV and 1.4 eV, respectively. With decreasing temperature, there are large changes in the phonon modes and the spectral weights are transferred to higher energy. Below the charge ordering temperature, the polaron absorption is suppressed and an optical gap starts to appear. The optical gap initially increases with decreasing temperature; however, it starts to decrease near 120 K. Our x-ray diffraction measurements show an increase of the a axis lattice constant below 120 K. These results suggest the importance of the lattice degrees of freedom for stabilizing the charge ordering in $La_{3/2}Sr_{1/2}NiO_4$.

DOI: 10.1103/PhysRevB.64.165106 PACS number(s): 71.45.Lr, 78.30.−j, 71.20.−b, 75.50.Ee

I. INTRODUCTION

The physical properties of $La_{2-x}Sr_xNiO_4$ have been investigated by many workers due to their close similarities with $La_{2-x}Sr_xCuO_4$ and the possibility of observing high-temperature superconductivity. Both parent compounds, i.e., La_2NiO_4 and La_2CuO_4, are antiferromagnetic insulators in their ground states. However, their physical properties with Sr doping have been shown to be quite different. While the cuprates show high-temperature superconductivity for $x \geqslant 0.05$, the nickelates do not show superconductivity for any x. And metallic conductivity appears much more slowly in the nickelates than the cuprates with respect to the hole doping, i.e., $x \geqslant 1.0$ in $La_{2-x}Sr_xNiO_4$ and $x \geqslant 0.05$ in $La_{2-x}Sr_xCuO_4$.[1] Such a self-localizing behavior of the holes has been attributed to a strong electron-phonon coupling and a strong magnetic localization in the nickelates.[2,3]

Using a neutron scattering experiment, Tranquada *et al.* proposed a stripe phase, which includes charge and spin ordering, to explain the magnetic and nuclear superlattice peaks in insulating $La_2NiO_{4.125}$.[4] The stripe phase has been observed for a wide range of hole doping, i.e., $0.2 \leqslant x \leqslant 0.5$ in $La_{2-x}Sr_xNiO_4$,[5] where the holes tend to segregate into stripes and form antiphase domain walls between the intervening antiferromagnetic regions. Especially, Chen, Cheong, and Cooper[6] reported evidence of quasi-two-dimensional (quasi-2D) charge modulations in $x=1/3$ and 1/2 at low temperature in their electron diffraction studies. According to their observations, it has been suggested that the hole stripes in $x=1/3$ and 1/2 should be located every third and every other Ni site, respectively. This work suggests the importance of the coupling between the ordered holes and the crystal lattice in producing the commensurate states.

Optical studies have proved to be quite useful for investigations of electron-phonon coupling and the electronic structures of several strongly correlated systems. There have been numerous reports on the optical properties of $La_{2-x}Sr_xNiO_4$ (Refs. 7–10); however, most of these studies have concentrated on samples with $x \leqslant 1/3$. Moreover, the role of lattice degrees of freedom on the stability of charge ordering and the detailed electronic structure near the Fermi level are not clearly understood yet.

In this paper, we report temperature- and polarization-dependent optical conductivity spectra $\sigma(\omega)$ of $La_{3/2}Sr_{1/2}NiO_4$. (Hereafter, $E\|ab$ and $E\|c$ indicate the fact that the light polarization is pointing along the ab plane and the c axis, respectively.) At room temperature, $\sigma(\omega)$ show broad peaks below 2.5 eV for $E\|ab$ and a peak around 3.3 eV for $E\|c$. We find that $\sigma(\omega)$ for $E\|ab$ originate from small polaron absorption and optical transitions between Ni $3d$ levels. Based on our assignments, we obtain the values of the crystal field splitting energy between e_g orbitals (~ 0.7 eV) and Hund's rule exchange energy (~ 1.4 eV), which are consistent with other experimental results.[11,12] With decreasing temperature, the small polaron absorption is suppressed and a large amount of spectral weights move to a higher energy. Below the charge ordering temperature T_{CO} ~ 240 K, a clear optical gap and changes of phonon structure can be observed for $E\|ab$. However, the optical gap starts to decrease below 120 K. This intriguing behavior

might be related to the fact that the lattice constant along the *a* axis seems to increase, indicating the importance of lattice degrees of freedom for stabilizing the charge ordering in $La_{3/2}Sr_{1/2}NiO_4$.

II. EXPERIMENTS

The $La_{3/2}Sr_{1/2}NiO_4$ single crystal was grown by the floating zone method. Details of crystal growth and characterization will be reported elsewhere.[13] Temperature-dependent dc resistivities for the ab plane, ρ_{ab}, and along the c axis, ρ_c, were measured using the four-probe method. For the measurement, the sample was cut into a rectangular shape and electrical contacts were made with a heat treatment of silver paint. High-resolution x-ray diffraction measurement was performed using the synchrotron radiation source at the Pohang Light Sources. The temperature-dependent lattice constants were obtained using a closed-cycle He refrigerator.

Just before the optical measurements, the sample was polished up to 0.1 μm using diamond paste. The temperature- and polarization-dependent reflectivity spectra were measured from 5 meV to 6 eV. For the energy regions of 5–20 eV, we used highly polarized light from the synchrotron radiation source to measure the polarization-dependent reflectivity spectra at room temperature. Kramers-Kronig analysis was used to obtain $\sigma(\omega)$. Details of the reflectivity measurements and the Kramers-Kronig transformation were reported elsewhere.[14] We also independently measured optical constants for the energy regions of 0.6–5 eV using spectroscopic ellipsometry. Since the optical constants of $La_{3/2}Sr_{1/2}NiO_4$ are anisotropic, we should measure the ratios of reflectances for *p*- and *s*-polarized light at several incident angles with the incident plane of the light along one of the optical axes of the sample, and then calculate the optical constants.[15] It was found that the data from the spectroscopic ellipsometry measurements agreed quite well with the results of our Kramers-Kronig analysis.

III. RESULTS AND DISCUSSIONS

Figure 1 shows the electrical characteristics of $La_{3/2}Sr_{1/2}NiO_4$. The solid and the dashed lines in Fig. 1(a) represent ρ_{ab} and ρ_c, respectively. In most of the measured temperature region, relatively large anisotropies between ρ_{ab} and ρ_c can be seen. With decreasing temperature, both ρ_{ab} and ρ_c increase, which is a typical insulator response. Figure 1(b) shows the curve of $\ln \rho_{ab}$ vs $1/T$, whose slope corresponds to the activation energy E_a. Clearly, there is a change of E_a around 240 K: the value of E_a changes from 0.068 to 0.121 eV. Its temperature, i.e., 240 K, corresponds to the charge ordering temperature, T_{CO}. Note that this single-crystal value is smaller than that reported in a polycrystalline sample, i.e., 340 K.[16] To our surprise, we find that the value of E_a changes once more from 0.121 to 0.063 eV near 120 K ($\equiv T_S$). Since the charge ordering is already stabilized at this lower temperature, the decrease of E_a is quite unusual. Later, we will show that this change might be related to an increase of the *a*-axis lattice constant.

Figures 2(a) and 2(b) show the temperature-dependent lattice constants for the *a* and the *c* axes, respectively. The error bars around 120 and 150 K are larger than those at other temperatures, since we determined independently the lattice constants at these temperatures using a conventional x-ray apparatus. The room-temperature lattice constants for the *a* and *c* axes are 3.820 Å and 12.724 Å, respectively. With decreasing temperature, the lattice constants start to decrease without apparent changes near T_{CO}, which is similar to the $La_{5/3}Sr_{1/3}NiO_4$ case.[17] However, the *a* axis lattice constant starts to increase near T_S, while the *c* axis lattice constant continues to decrease without any noticeable changes. Be-

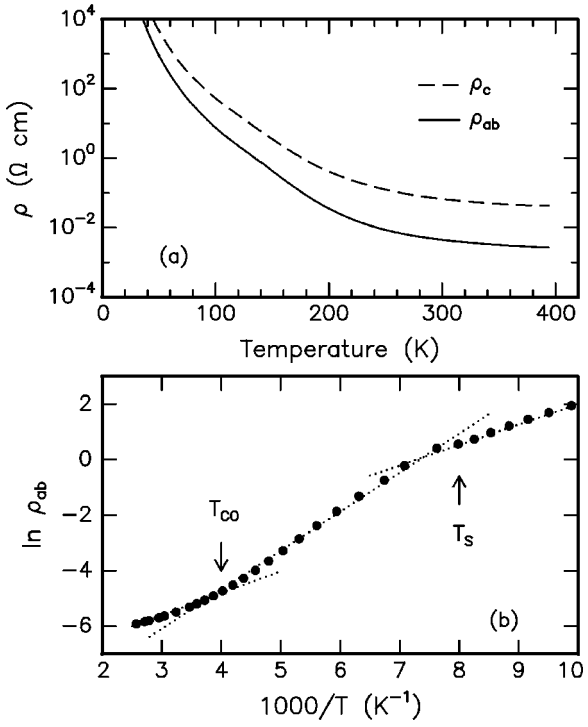

FIG. 1. (a) Temperature-dependent dc resistivities for the *ab* plane, ρ_{ab} (solid line), and along the *c* axis, ρ_c (dashed line). (b) Curve of $\ln \rho_{ab}$ vs $1/T$.

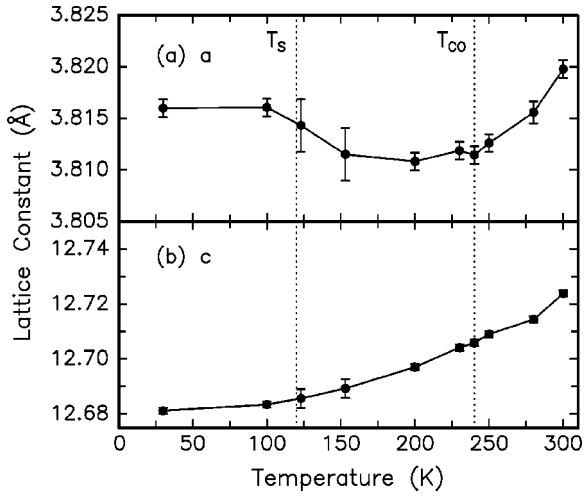

FIG. 2. Temperature-dependent lattice constants for the (a) *a* and (b) *c* axes.

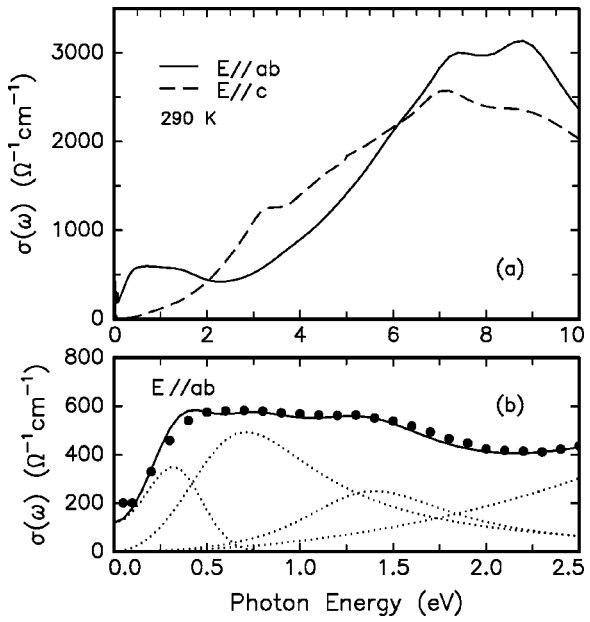

FIG. 3. (a) Polarization-dependent $\sigma(\omega)$ below 10 eV at 290 K. (b) Magnified $\sigma(\omega)$ for $E\|ab$ below 2.5 eV. In (b), the solid circles, the dotted lines, and the solid line represent the real data, the fitting lines, and the sum of the fitting lines, respectively.

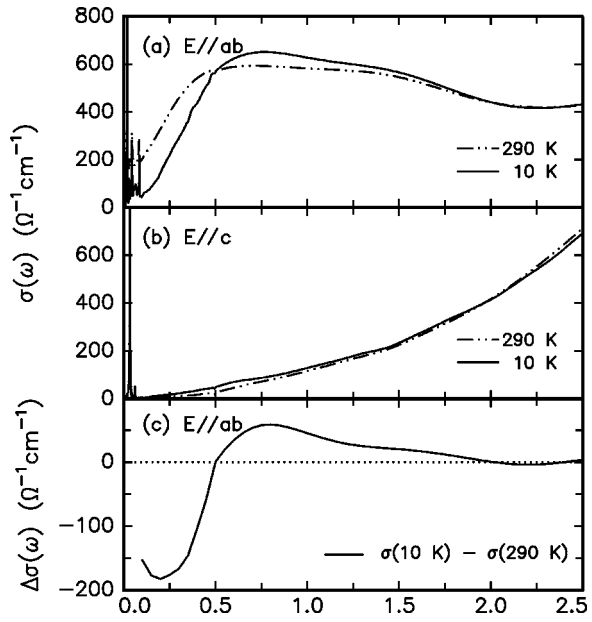

FIG. 4. Midinfrared $\sigma(\omega)$ at 10 and 290 K for (a) $E\|ab$ and (b) $E\|c$. In (c), $\Delta\sigma(\omega)$ $[\equiv\sigma(\omega,10\ \mathrm{K})-\sigma(\omega,290\ \mathrm{K})]$ is shown for $E\|ab$.

tween 100 and 200 K, the a axis lattice constant increases by about 0.137% and the c axis lattice constant decreases by about 0.107%. It is not clear whether this intriguing temperature dependence comes from a structural phase transition or not. Further studies on this point are highly desirable.

Optical conductivity spectra show a strong anisotropy in the low-energy region. Figure 3(a) shows $\sigma(\omega)$ at 290 K for two light polarizations. The solid and dashed lines represent $\sigma(\omega)$ for $E\|ab$ and $E\|c$, respectively. Above 5.0 eV, both spectra show two broad and strong peaks around 7.4 and 8.8 eV. These peaks were assigned as O $2p\rightarrow$Ni $3d$ and O $2p\rightarrow$La $5d/4f$ transitions,[18] which should be nearly polarization independent and dipole allowed. On the other hand, the low-energy peaks are rather weak and highly anisotropic. For $E\|ab$, $\sigma(\omega)$ show a broad peak below 2.5 eV and a steep rise above 3 eV. For $E\|c$, however, spectral weights below 2.5 eV are negligible, and the first peak appears around 3.3 eV.

There have been several works which have considered the origins of the ab plane peaks below 2.5 eV. Ido *et al.*[19] reported two broad absorption peaks around 0.6 eV and 1.5 eV in $\sigma(\omega)$ of $La_{2-x}Sr_xNiO_4$ $(0.1\leqslant x\leqslant 0.5)$ and suggested that they should be related to the symmetry of the doped holes. Bi *et al.*[7] investigated the midinfrared absorption bands of the $0.05\leqslant x\leqslant 0.2$ samples and assigned them to photon-assisted hopping of the small polarons. The small polaron model could explain the rising region of $\sigma(\omega)$ quite well; however, it could not explain the $\sigma(\omega)$ above 0.5 eV. Recently, Tsutsui *et al.*[20] calculated $\sigma(\omega)$ for the doped nickelates by using the numerically exact diagonalization method. Using a Hamiltonian with electron hopping, on-site Coulomb interaction, and Hund's rule coupling between electrons in e_g orbitals, they found that 2D nickelates should have two absorption peaks in the low-energy region. (Note that electron-phonon interaction and crystal field splitting between e_g orbitals were neglected in their Hamiltonian.)

To understand the origins of the peaks below 2.5 eV, we investigated the temperature dependences of $\sigma(\omega)$ for $E\|ab$ and $E\|c$, which are shown in Figs. 4(a) and 4(b), respectively. While $\sigma(\omega)$ for $E\|c$ show little temperature dependences, those for $E\|ab$ show significant changes up to 2 eV. At 10 K, $\sigma(\omega)$ for $E\|ab$ show an optical gap and a significant amount of spectral weight below 0.5 eV is transferred to higher energy. These differences in $\sigma(\omega)$ with respect to temperature are quite consistent with a recent result that charge ordering should occur within the NiO_2 planes and charge ordering correlation along the c axis should be nearly absent.[6] Figure 4(c) shows the difference of $\sigma(\omega)$ between 10 and 290 K, i.e., $\Delta\sigma(\omega)[\equiv\sigma(\omega,10\ \mathrm{K})-\sigma(\omega,290\ \mathrm{K})]$ for $E\|ab$. (For clarity, $\Delta\sigma(\omega)$ below 0.1 eV is omitted.) Clearly, the most significant spectral weight changes occur below 0.5 eV, near 0.75 eV, and near 1.5 eV. The sum of missed spectral weights below 0.5 eV is nearly the same as that of increased spectral weights between 0.5 and 2.0 eV. This satisfaction of the optical sum rule suggests that most of the related electronic structure changes occur near the Fermi energy.

The lowest spectral weight changes may be due to the small polaron absorption. Many optical results[7–9] on $La_{2-x}Sr_xNiO_4$ with $x\leqslant 1/3$ have suggested the existence of the small polaron at high temperature due to the strong electron-phonon interaction.[21,22] Even for our sample with $x=1/2$, the small polaron absorption is the most plausible picture. Then, the negative value of $\Delta\sigma(\omega)$ below 0.5 eV can be explained by the suppression of the small polaron absorption due to the charge ordering.

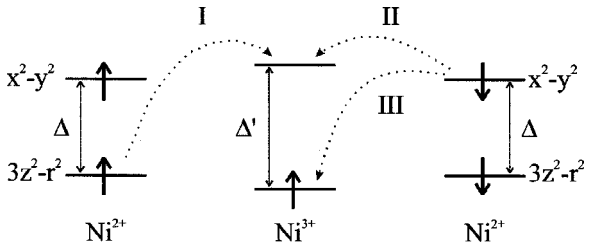

FIG. 5. Schematic diagram of the optical transitions, and the electronic configurations of Ni^{2+} and Ni^{3+} ions.

Keeping in mind the existence of three peaks below 2.5 eV, we fitted $\sigma(\omega)$ below 2.5 eV, using the functional forms of the small polaron and the Lorentz oscillators, i.e.,

$$\sigma(\omega)=\sigma_{dc}\frac{\sinh(\hbar\omega/2k_BT)}{\hbar\omega/2k_BT}\exp[-(\hbar\omega)^2/8E_bk_BT]$$

$$+\sum_i \frac{S_i\Gamma_i\omega^2}{(\omega^2-\omega_i^2)^2+\Gamma_i^2\omega^2}. \quad (1)$$

The first term corresponds to the small polaron absorption, and σ_{dc} and E_b represent the dc conductivity and the polaron binding energy, respectively.[23] The second term denotes a sum of the Lorentz oscillators, where S_i, Γ_i, and ω_i represent the strength, the damping constant, and the energy of the ith Lorentz oscillator, respectively. For the small polaron fitting, we used the value of $\sigma_{dc}=120\ \Omega^{-1}\,\mathrm{cm}^{-1}$ and $E_b=0.19$ eV. It is known that the value of E_b should be 2 times larger than that of E_a.[23] The fitting parameter of 0.19 eV is somewhat larger than 0.14 eV ($\sim 2\times 0.068$ eV) for E_b. Similar results were previously noticed for the $La_{2-x}Sr_xNiO_4$ ($0.05\leqslant x\leqslant 0.2$) samples by Bi *et al.*[7] For the Lorentz oscillator fitting, we first subtract the contribution from the charge transfer transition above 2 eV, and then fit the remaining $\sigma(\omega)$ using two Lorentz oscillators centered around 0.71 and 1.4 eV. As shown in Fig. 3(b), this fitting result can explain the experimental $\sigma(\omega)$ quite well.

To understand these two peaks, we considered the electronic configurations of the Ni^{2+} and the Ni^{3+} ions, as shown in Fig. 5. In $Ni^{2+}(3d^8)$, six electrons fill t_{2g} levels and two electrons fill e_g levels. The electrons in the e_g levels have $d_{3z^2-r^2}$ and $d_{x^2-y^2}$ orbitals, and have the same spins due to the large Hund's rule exchange energy. Since the in-plane Ni-O bonding length is different from the out-of-plane bonding length, the $d_{3z^2-r^2}$ and the $d_{x^2-y^2}$ levels are split by Δ. On the other hand, in $Ni^{3+}(3d^7)$, six electrons fill the t_{2g} levels and one electron fills the e_g level with $d_{3z^2-r^2}$ orbital.[24] Since one electron fills in e_g level with $d_{3z^2-r^2}$ orbital in Ni^{3+}, there could be an additional Jahn-Teller-like distortion.[25] (In fact, the lattice constant ratio between c and a axes, i.e., c/a, has been known to be increased up to $x=1/2$ in $La_{2-x}Sr_xNiO_4$.[17]) Therefore, the level splitting between the $d_{3z^2-r^2}$ and the $d_{x^2-y^2}$ in the Ni^{3+} ion (Δ') could be slightly larger than Δ. And the difference between Δ' and Δ might be similar to E_a.[26]

Among numerous intersite optical transitions between Ni^{2+} and Ni^{3+} ions, we considered three optical transitions which are displayed in Fig. 5. (Other optical transitions may exist above 2.5 eV or have small optical strengths.) Transition I corresponds to an optical transition between Ni^{2+} and Ni^{3+} ions with the same spin direction. The electron in the filled $d_{3z^2-r^2}$ ($\uparrow$) level in Ni^{2+} site moves to the unfilled $d_{x^2-y^2}$ level in Ni^{3+} site, and it requires an energy of about $(\Delta'+\Delta)/2$. Transitions II and III correspond to optical transitions between Ni^{2+} and Ni^{3+} ions with the opposite spin direction. In transition II, the electron in the filled $d_{x^2-y^2}$ ($\downarrow$) level in the Ni^{2+} site moves to the unfilled $d_{x^2-y^2}$ level in the Ni^{3+} site, and it requires an energy of about $J+(\Delta'-\Delta)/2$. (Here J represents the Hund's rule exchange energy.) In transition III, the electron in the filled $d_{x^2-y^2}$ ($\downarrow$) level in the Ni^{2+} site moves to the filled $d_{3z^2-r^2}$ ($\uparrow$) level in the Ni^{3+} site, and it requires an energy of about $J-(\Delta'+\Delta)/2$. It is expected that the strengths of transitions I and III may be smaller than that of transition II, since the former transitions occur between different types of orbitals, i.e., $d_{3z^2-r^2}$ and $d_{x^2-y^2}$, and the latter occurs between the same types of orbitals, i.e., $d_{x^2-y^2}$.

As mentioned earlier, the optical data seem to be fitted quite well with two Lorentz oscillators centered around 0.71 and 1.4 eV. The strength of the first Lorentz oscillator is larger than that of the second one. Comparing with the energies and the strengths of transitions I, II, and III, we claim that the first Lorentz oscillator might come from the sum of transitions I and III, and the second one comes from transition II. From these assignments, we can extract the approximate value of $\Delta\sim 0.7$ eV and $J\sim 1.4$ eV.[27] These values are quite consistent with recent experimental results. Kuiper *et al.*[11] obtained a similar value of Δ using the polarization-dependent x-ray absorption spectra at the nickel L edges in La_2NiO_4. Pellegrin *et al.*[12] investigated the polarization-dependent O $1s$ x-ray absorption measurement on $La_{2-x}Sr_xNiO_4$ ($0\leqslant x\leqslant 0.6$). For $E\|ab$, they observed peaks at 528.7 and 530 eV, and assigned as the high-spin ($|d_{x^2-y^2}\uparrow d_{3z^2-r^2}\uparrow\rangle$) and the low-spin $[(1/\sqrt{2})\times(|d_{x^2-y^2}\uparrow d_{3z^2-r^2}\downarrow\rangle-|d_{x^2-y^2}\downarrow d_{3z^2-r^2}\uparrow\rangle)]$ states, respectively. The energy difference (~ 1.3 eV) between these states may correspond to J.

It would be helpful to compare our assignments with those done by Tsutsui *et al.*[20] They calculated $\sigma(\omega)$ of the doped nickelates from a Hamiltonian which does not include Δ. They obtained two broad peaks in $\sigma(\omega)$, and assigned the first peak as originating from the hopping of the electron which disturbed the spin configuration, and the second peak as from the excitation in which the motion of carrier changed doubly occupied sites from high-spin to low-spin states. Although Δ is much smaller than the on-site Coulomb repulsion, it is still comparable to the low-energy excitations observed in Fig. 3(b). Therefore, we think that our assignments which consider the role of Δ are more plausible.

Figures 6(a) and 6(b) show the temperature-dependent optic phonon modes for $E\|ab$ and $E\|c$, respectively. At 290 K, $\sigma(\omega)$ for $E\|ab$ show four optic phonon modes, centered around 149, 234, 361, and 667 cm^{-1}, and those for $E\|c$ show two optic phonon modes, centered around 262 and 491 cm^{-1}. According to the group theory of La_2NiO_4 with

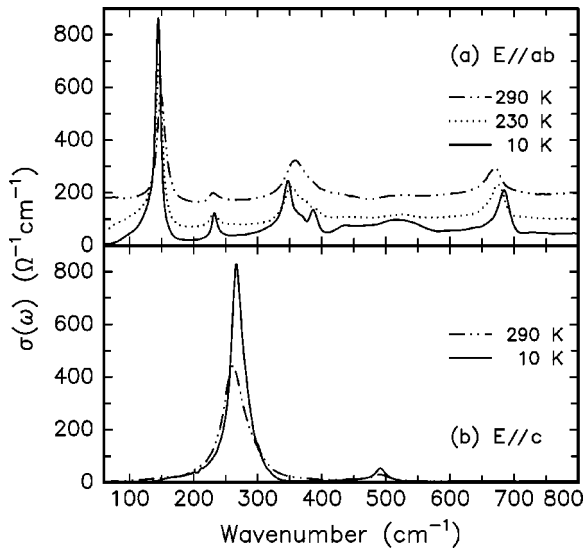

FIG. 6. Optic phonon modes for (a) $E\|ab$ and (b) $E\|c$ at some selected temperatures.

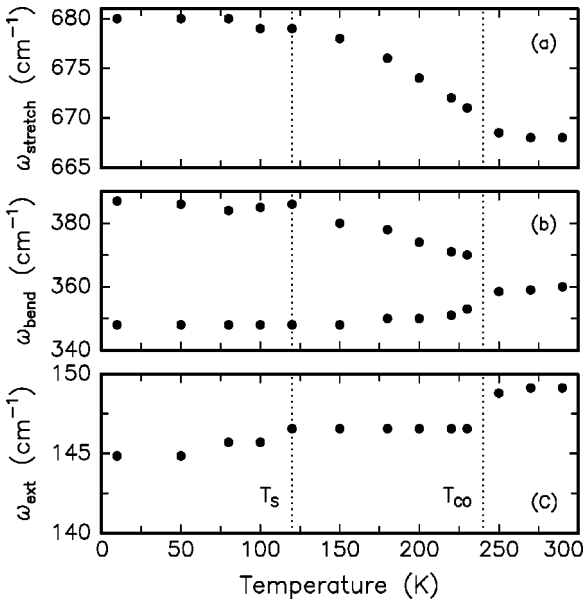

FIG. 7. Temperature-dependent frequencies of (a) the stretching ($\omega_{stretch}$), (b) the bending (ω_{bend}), and (c) the external (ω_{ext}) modes for $E\|ab$.

D_{4h}^{17} symmetry, four (three) infrared-active phonon modes are expected for $E\|ab$ ($E\|c$).[28] They correspond to one external, two bending, and one stretching mode for $E\|ab$ and one external, one bending, and one stretching mode for $E\|c$. For La_2NiO_4, Tajima *et al.*[29] reported four optic phonon modes centered around 150, 236, 367, and 675 cm^{-1} for $E\|ab$ and three modes centered around 280, 370, and 515 cm^{-1} for $E\|c$. In our $La_{3/2}Sr_{1/2}NiO_4$ sample, only two modes are apparently visible for $E\|c$ and all the frequencies are smaller than those for La_2NiO_4. These differences of phonon modes between La_2NiO_4 and $La_{3/2}Sr_{1/2}NiO_4$ might be due to the change of the lattice constant or the change of local symmetry with doping.

With decreasing temperature, for $E\|ab$, the broad background of $\sigma(\omega)$ decreases and the phonon modes become clear. In particular, the bending mode located around 361 cm^{-1} starts to split and the stretching mode located around 667 cm^{-1} moves significantly to higher frequency just below $T_{CO}\sim 240$ K. The changes of the optic phonon modes near T_{CO} suggest that the charge ordering should be coupled with the local lattice distortion. For $E\|c$, the phonon mode located around 262 cm^{-1} becomes sharper and slightly moves to higher frequency. No significant changes, such as bending mode splitting and a shift of the stretching mode, can be observed. To obtain more quantitative information on the temperature-dependent optic phonon modes, we fit them with Lorentz oscillators and summarize the fitting parameters for $E\|ab$ and $E\|c$ in Table I.

Figures 7(a), 7(b), and 7(c) show the temperature-dependent frequencies of the stretching ($\omega_{stretch}$), the bending (ω_{bend}), and the external (ω_{ext}) modes for $E\|ab$, respectively. Above T_{CO}, there are little changes. Below T_{CO}, $\omega_{stretch}$ moves to a higher frequency by about 15 cm^{-1}, and ω_{ext} shifts to a lower frequency by about 3 cm^{-1}. In addition, one of the split bending mode moves to higher frequency and the other moves to the opposite. It seems that T_S is another important temperature where the temperature dependences of the phonon frequency change. Below T_S, the shifts of the bending and the stretching modes seem to be

TABLE I. The phonon parameters of $La_{3/2}Sr_{1/2}NiO_4$ at 290 and 10 K for $E\|ab$ and $E\|c$.

$E\|ab$						$E\|c$					
ω_i (cm^{-1})		Γ_i (cm^{-1})		S_i (Ω^{-1} cm^{-1} cm^{-1})		ω_i (cm^{-1})		Γ_i (cm^{-1})		S_i (Ω^{-1} cm^{-1} cm^{-1})	
290 K	10 K	290 K	10 K	290 K	10 K	290 K	10 K	290 K	10 K	290 K	10 K
149.1	144.4	15.6	10.8	6491	9249	262.3	267.9	43.8	26.5	19055	21209
233.6	234.1	21.9	31.5	789	2597						
	346.7		35.9		7100						
360.5	386.9	49.9	12.4	7721	1026						
	441.9		47.2		1515	490.6	490.9	27.9	20.2	679	990
	523.1		133.8		12079						
667.2	682.6	33.1	29.4	3390	5302						

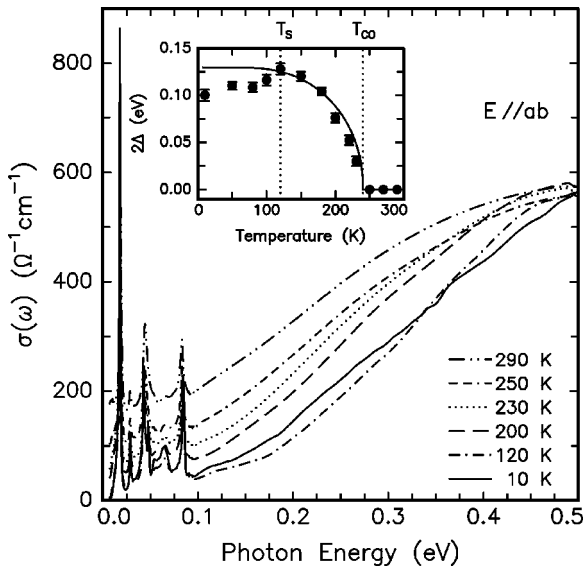

FIG. 8. Temperature-dependent $\sigma(\omega)$ for $E\|ab$ below 0.5 eV. In the inset, values of optical gap (2Δ) are shown. The solid line is the BCS functional form.

saturated. Also, ω_{ext} shows an additional shift of about 2 cm^{-1} at this temperature. Another interesting fact is that the shifts of $\omega_{stretch}$ and ω_{bend} are quite large, i.e., about 15 cm^{-1}. Such a large value of the phonon shift cannot be explained solely by the changes of the lattice constants. For $La_{0.7}Ca_{0.3}MnO_3$ and $La_{1/2}Sr_{3/2}MnO_4$, similar changes were observed and attributed to other degrees of freedom, such as the strong electron-phonon coupling and/or the intersite Coulomb repulsion.[30,31]

The importance of T_S can be also observed in the temperature dependent-spectral weight changes for $E\|ab$ below 0.5 eV, shown in Fig. 8. At 290 K, $\sigma(\omega)$ show the midinfrared feature due to the small polaron absorption. In the dc limit (i.e., $\omega\rightarrow 0$), $\sigma(\omega)$ approach a finite value, which agrees with the experimental value of the dc conductivity. Since it is an insulating state, the strong Drude peak cannot be observed. With decreasing temperature, the spectral weights below 0.5 eV decrease and move to the higher energy. Below T_{CO}, $\sigma(\omega)$ in the low-frequency region become strongly suppressed and an optical gap starts to appear. The spectral weight suppression becomes largest around T_S. It is quite clear that $\sigma(\omega)$ below 0.35 eV at 10 K is larger than those at 120 K. (Since the amount of spectral weight changes between 10 K and 120 K are rather small, we measured the optical reflectivity spectra several times and found that such intriguing behavior was quite reproducible.)

To get further understanding, we evaluated the values of optical gap 2Δ from the crossing points of abscissa with linear extrapolations of $\sigma(\omega)$. As shown in the inset of Fig. 8, 2Δ shows an interesting change near T_S. With decreasing temperature, 2Δ starts to appear at T_{CO} and becomes steeply increased. However, below T_S, 2Δ becomes decreased: $\sim$0.1 eV at 10 K (Ref. 32) and $\sim$0.13 eV at 120 K. The solid line is the temperature dependence of 2Δ with a BCS functional form. The BCS functional form has been used for the temperature dependence of gap values for the charge-density-wave and the spin-density-wave transitions.[33] A clear deviation of 2Δ from the BCS functional form occurs at T_S. Note that such a behavior has not been reported in $La_{5/3}Sr_{1/3}NiO_4$.[8]

As yet, the decrease of 2Δ below T_S is not clearly understood. However, the increase of the lattice constant for the a axis below T_S will be an important clue. When the lattice constant increases, the distance between the hole stripes should also increase. Then, the interaction such as Coulomb repulsion between the hole stripes will decrease. Since the electron fills the $d_{3z^2-r^2}$ orbital (and the hole in the $d_{x^2-y^2}$ orbital) in the hole stripe of the Ni^{3+} site, it is also likely that the electron with the $d_{3z^2-r^2}$ orbital (also the hole with the $d_{x^2-y^2}$ orbital) will be unstable. And an antiferromagnetic exchange interaction between the spins in the Ni sites will also decrease. The combined effects of such phenomena can result in a decrease of 2Δ below T_S. Although more systematic studies are needed, our results suggest that there might be a strong correlation between the stabilization of charge ordering and the lattice degrees of freedom in $La_{3/2}Sr_{1/2}NiO_4$.

IV. SUMMARY

We have investigated the temperature- and polarization-dependent optical conductivity spectra of $La_{3/2}Sr_{1/2}NiO_4$, which undergoes a charge ordering below $T_{CO}\sim 240$ K. The optical conductivity spectra show strong anisotropies in both the optic phonon modes and the electronic structures between the ab plane and the c axis. With variations of temperature, the phonon modes are significantly changed and large changes of the electronic structures are observed for the ab plane. However, these show little temperature dependences along the c axis. In the midinfrared region, for the ab plane, we find that there are several peaks due to a small polaron absorption and optical transitions between e_g levels in neighboring Ni sites. Below T_{CO}, the small polaron absorption is suppressed and an optical gap starts to appear. The optical gap increases but suddenly decreases with the increase of the a axis lattice constant near 120 K. This intriguing behavior suggests that there might be a strong correlation between the stabilization of charge ordering and the lattice degrees of freedom in $La_{3/2}Sr_{1/2}NiO_4$.

ACKNOWLEDGMENTS

We acknowledge Professor Y. K. Bang, Professor Jaejun Yu, and Professor B. J. Suh for helpful discussions and J. H. Park and Professor K.-B. Lee for their help in synchrotron x-ray diffraction measurements. This work was supported by the Ministry of Science and Technology through the Creative Research Initiative Program, and it was also supported by the Korea Science and Engineering Foundation through the CSCMR at Seoul National University. Experiments at PLS were supported in part by MOST and POSCO. And work at Korea Basic Science Institute was supported by the National Research Laboratory project of the Korean Ministry of Science and Technology. One of us (G.B.) would like to thank the EPSRC, UK, for financial support.

*Current address: Samsung Advanced Institute of Technology, P.O. Box 111, Suwon, Kyongki 440-600, Korea.
†Current address: Institute Laue Langevin, BP156 38042 Grenoble, France.
[1] R.J. Cava, B. Batlogg, T.T. Palstra, J.J. Krajewski, W.F. Peck, A.P. Ramirez, and L.W. Rupp, Phys. Rev. B **43**, 1229 (1991) and references therein.
[2] V.I. Anisimov, M.A. Korotin, J. Zaanen, and O.K. Andersen, Phys. Rev. Lett. **68**, 345 (1992).
[3] J. Zannen and P.B. Littlewood, Phys. Rev. B **50**, 7222 (1994).
[4] J.M. Tranquada, D.J. Buttrey, V. Sachan, and J.E. Lorenzo, Phys. Rev. Lett. **73**, 1003 (1994).
[5] S.M. Hayden, G.H. Lander, J. Zzarestky, P.J. Brown, C. Stassis, P. Metcalf, and J.M. Honig, Phys. Rev. Lett. **68**, 1061 (1992); S.-H. Lee and S-W. Cheong, *ibid.* **79**, 2514 (1997); H. Yoshizawa, T. Kakeshita, R. Kajimoto, T. Tanabe, T. Katsufuji, and Y. Tokura, Phys. Rev. B **61**, R854 (2000).
[6] C.H. Chen, S-W. Cheong, and A.S. Cooper, Phys. Rev. Lett. **71**, 2461 (1993).
[7] X-X. Bi, P.C. Eklund, and J.M. Honig, Phys. Rev. B **48**, 3470 (1993); X-X. Bi and P.C. Eklund, Phys. Rev. Lett. **70**, 2625 (1993).
[8] T. Katsufuji, T. Tanabe, T. Ishikawa, Y. Fukuda, T. Arima, and Y. Tokura, Phys. Rev. B **54**, 14 230 (1996).
[9] P. Calvani, A. Paolone, P. Dore, S. Lupi, P. Maselli, P.G. Medaglia, and S-W. Cheong, Phys. Rev. B **54**, R9592 (1996).
[10] Y.G. Pashkevich, V.A. Blinkin, V.P. Gnezdilov, V.V. Tsapenko, V.V. Eremenko, P. Lemmens, M. Fischer, M. Grove, G. Güntherodt, L. Degiorgi, P. Wachter, J.M. Tranquada, and D.J. Buttrey, Phys. Rev. Lett. **84**, 3919 (2000).
[11] P. Kuiper, J. van Elp, D.E. Rice, D.J. Buttrey, H.-J. Lin, and C.T. Chen, Phys. Rev. B **57**, 1552 (1998).
[12] E. Pellegrin, J. Zaanen, H.-J. Lin, G. Meigs, C.T. Chen, G.H. Ho, H. Eisaki, and S. Uchida, Phys. Rev. B **53**, 10 667 (1996).
[13] G. Balakrishnan *et al.* (unpublished).
[14] J.H. Jung, K.H. Kim, D.J. Eom, T.W. Noh, E.J. Choi, J. Yu, Y.S. Kwon, and Y. Chung, Phys. Rev. B **55**, 15 489 (1997); K.H. Kim, J.H. Jung, and T.W. Noh, Phys. Rev. Lett. **81**, 1517 (1998).
[15] R.M.A. Azzam and N.M. Bashara, *Ellipsometry and Polarized Light* (Elsevier Science, Amsterdam, 1989).
[16] S-W. Cheong, H.Y. Hwang, C.H. Chen, B. Batlogg, L.W. Rupp, Jr., and S.A. Cater, Phys. Rev. B **49**, 7088 (1994).
[17] S.H. Han, M.B. Maple, Z. Fisk, S-W. Cheong, A.S. Cooper, O. Chmaissem, J.D. Sullivan, and M. Marezio, Phys. Rev. B **52**, 1347 (1995).
[18] S. Tajima, H. Ishii, T. Nakahashi, T. Takagi, S. Uchida, M. Seki, S. Suga, Y. Hidaka, M. Suzuki, T. Murakami, K. Oka, and H. Unoki, J. Opt. Soc. Am. B **6**, 475 (1989).
[19] T. Ido, K. Magoshi, H. Eisaki, and S. Uchida, Phys. Rev. B **44**, 12 094 (1991).
[20] K. Tsutsui, W. Koshibae, and S. Maekawa, Phys. Rev. B **59**, 9729 (1999).
[21] Y-S. Yi, Z-G. Yu, A.R. Bishop, and J.T. Gammel, Phys. Rev. B **58**, 503 (1998).
[22] R.J. McQueeney, J.L. Sarrao, and R. Osborn, Phys. Rev. B **60**, 80 (1999).
[23] I.J. Austin and N.F. Mott, Adv. Phys. **18**, 41 (1969); H.G. Reik and D. Heese, J. Phys. Chem. Solids **28**, 581 (1967); R. Mülstroh and H.G. Reik, Phys. Rev. **162**, 703 (1967).
[24] A. Sahiner, M. Croft, Z. Zhang, M. Greenblatt, I. Perez, P. Metcalf, H. Jhans, G. Liang, and Y. Jeon, Phys. Rev. B **53**, 9745 (1996).
[25] J. Gopalakrishnan, G. Colsmann, and B. Reuter, J. Solid State Chem. **22**, 145 (1977).
[26] P. A. Cox, *Transition Metal Oxides* (Clarendon Press, Oxford, 1992).
[27] Since values of Δ and Δ' are one order of magnitude larger than E_a, $\Delta \sim \Delta'$. Due to the broadness of our Lorentz oscillators, it would be difficult to obtain more accurate values of Δ and Δ'.
[28] L. Pintschovius, J.M. Bassat, P. Odier, F. Gervais, G. Chevrier, W. Reichardt, and F. Gompf, Phys. Rev. B **40**, 2229 (1989).
[29] S. Tajima, T. Ido, S. Ishibashi, T. Ito, H. Eisaki, Y. Mizuo, T. Arima, H. Takagi, and S. Uchida, Phys. Rev. B **43**, 10 496 (1999).
[30] K.H. Kim, J.Y. Gu, H.S. Choi, G.W. Park, and T.W. Noh, Phys. Rev. Lett. **77**, 1877 (1996).
[31] J.H. Jung, H.J. Lee, T.W. Noh, and Y. Moritomo, J. Phys.: Condens. Matter **12**, 9799 (2000).
[32] The 2Δ value at 10 K was reported to be around 0.25 eV in $La_{5/3}Sr_{1/3}NiO_4$ (Ref. 8). This result might imply that the charge ordering is more stable for $x=1/3$ than for $x=1/2$, as consistent with recent dc resistivity measurement at high electric field [S. Yamanouchi, Y. Taguchi, and Y. Tokura, Phys. Rev. Lett. **83**, 5555 (1999)].
[33] A.W. Overhauser, Phys. Rev. **128**, 1437 (1962); **167**, 691 (1968).